# New Projected Rotational Velocity Measurements for 65 Mid M-Dwarfs

**Cassy L. Davison[1], R.J. White[1], T.J. Henry[1], N. Cabrera[1]**

[1] *Georgia State University, Department of Physics and Astronomy, Atlanta, GA, 30303, USA*

**Abstract.** To determine how the projected rotational velocity ($v\sin i$) of a M-star changes with spectral type, we assembled a list of all known single (within 2″) mid to late M-dwarfs that have trignometric parallaxes within 25 pc and reside between −30° and +65° Decl. From this list of 408 stars, only 166 stars have reported $v\sin i$ values. To gain a more complete and less biased census of the population, we obtained new spectroscopic measurements for an additional 65 stars, yielding an increase in known $v\sin i$ values by 39%. Our data indicate the frequency of mid M-dwarfs with a $v\sin i$ value greater than 3 km s$^{-1}$ may be lower than previously thought. Also, our data indicate that close to ∼60% of the late M-dwarfs (M6-M9) have $v\sin i$ values below 10 km s$^{-1}$ and are viable candidates to search for low mass planets with the radial velocity technique.

## 1. Introduction

The 2010 decadal survey, "New Worlds, New Horizons in Astronomy and Astrophysics," challenged the astronomical community to develop new and innovative technology to identify Earth-mass planets in the habitable zones of nearby stars using the Doppler technique. Since M-dwarfs are the most ubiquitous stars (∼75% of field stars; Henry et al. 2014), they are the most likely to harbor the nearest habitable planets (e.g. Swift et al. 2013; Dressing & Charbonneau 2013). To facilitate these potential discoveries, modern spectrographs are being designed and built (including Habitable Zone Planet Finder, SPIRou, CARMENES and iSHELL with use of a gas cell; Mahadevan et al. 2012; Reshetov et al. 2012; Quirrenbach et al. 2010; Rayner et al. 2012) that will have the capability to achieve ∼1−10 m s$^{-1}$ single-measurement precision for faint low mass stars. These RV precisions will allow terrestrial planets to be found in the habitable zone of slowly-rotating, inactive, single, nearby low mass stars (mid to late M-dwarfs).

Along with brightness, the achievable radial velocity accuracy strongly depends on rotational broadening. One of the largest surveys of M-dwarfs has instituted the criteria that their target stars must have vsini < 6.5 km s$^{-1}$ in order to be viable candidates for planet searches (Bonfils et al. 2013). This criteria does not affect most early M-dwarfs (M0-M3), as these stars are usually slow rotators with vsini < 3 km s$^{-1}$ (Marcy & Chen 1992; Browning et al. 2010; Reiners et al. 2012). However, initial surveys reveal that mid and late M-dwarfs that will be surveyed by the

next generation spectrographs are not quiet stars and tend to have higher rotational velocities (e.g. Mohanty & Basri 2003; Reiners & Basri 2008; Jenkins et al. 2009). With preliminary surveys indicating that many late type stars have high rotational velocities, it becomes evident that we need to obtain rotational velocities for all of the nearest stars to determine which stars are suitable for future radial velocity monitoring.

## 2. Sample

In an effort to obtain unbiased statistics on how projected rotational velocity values for mid to late mid M-dwarfs vary with spectral type, we assembled our sample from the REsearch Consortium On Nearby Stars (RECONS) 25 Parsec Database (Henry et al. 2014) of 3074 stars, brown dwarfs, and exoplanets in 2168 systems[1]. All of the stars in this database have published trignometric parallaxes greater than 40 milli-arcseconds (mas; d<25 pc) and errors below 10 mas. From this list, we selected all mid M-dwarfs that lie between $-30°$ and $+65°$ Decl. and do not have known companions within $2''$. We define mid to late M-dwarfs as stars with V-K values between 4.65 and 9.0 mag. We then excluded all spectroscopically determined brown dwarfs with spectral type of L0 or later. A total of 408 stars meet these criteria, yet only 166 of these stars have published projected rotational velocity values (Browning et al. 2010; Barnes et al. 2014; Davison et al. 2014; Delfosse et al. 1998; Jenkins et al. 2009; Jones et al. 2005; Mohanty & Basri 2003; Reiners & Basri 2007, 2010; Reiners et al. 2012; Stauffer & Hartmann 1986; Tanner et al. 2012).

Of the remaining 239 stars without published $v\sin i$ values, 149 of these stars are infrared bright ($K_S > 9$) and are easily observable with the 3-m telescope at NASA's Infrared Telescope Facility (IRTF).

## 3. Spectroscopy

### 3.1 Observations

We obtained spectra of 65 mid M-dwarfs using CSHELL (Tokunaga et al. 1990; Greene et al. 1993) on IRTF. CSHELL is a long-slit echelle spectrograph that utilizes a circular variable filter to isolate a single order. Our central wavelength is at 2.298 microns (vacuum) and spans approximately 50 Å. We use CSHELL in high resolution mode ($0.5''$; slit=2.5 pixels), which yields a resolving power of ∼40,000. We obtained data on 13 different nights between 2014 January and 2014 July. For each star, we obtained two spectra consecutively in two different positions along the slit; we later refer to these as nod positions. Our exposure times ranged from 600 to 1200 seconds per nod position, and were set to yield a signal to noise ratio (SNR) of 75 (or optimally a combined SNR of 100+). Along with the spectra of mid M-dwarfs, we also obtained spectra of telluric standards each night, which will be used to determine the instrumental profile of the CSHELL. Every night, we obtained 30 flats and 30 darks with an integration time of 20 seconds each.

### 3.2 Image Reduction and Spectral Extraction

A brief overview highlighting the many aspects and advantages of our spectral extraction and radial velocity fitting routine will be given here. For a full explanation of the data reduction technique the reader is referred to (Bailey et al. 2012; Davison et al. in prep.). To prepare the 2D images for spectral extraction, we start by subtracting each nodded pair of images from one another to

[1]3074 stars, brown dwarfs, and exoplanets in 2168 systems are included as of January 1, 2014.

remove dark current, sky emission and detector bias. Then, we correct each image for flat fielding using a master flat field image from all flat field images obtained on a particular night. We then apply a bad pixel mask to our spectra and set the spectral value to zero for all hot and dead pixels.

We optimally extract each spectrum following the procedures in Horne (1986) as implemented for nod-subtracted spectra in Bailey et al. (2012) tuned to work for CSHELL data (Davison et al. 2014). To obtain an optimally extracted spectrum, we sum the pixels of a nod-subtracted spectral image over the cross dispersion direction to obtain the standard spectrum. Next, we fit the spectral profile of the standard spectrum with a Gaussian and a second order polynomial to model our spatial profiles at each pixel step (column) along the order parallel to the dispersion direction of the image. From this, the variance of the spectrum's spatial profile is determined and then we weight the pixel values based on this profile. Then, we sum the weighted pixels to create our optimally extracted spectrum. For low signal to noise to data, we interpolate over pixels that are more than 5 sigma above or below the running average of the five pixels next to the pixel in question to remove any remaining deviant features.

To obtain an estimate of the signal to noise ratio (SNR) for each spectrum, we use a simplified version of the CCD equation from Mortara & Fowler (1981) modified to account for the noise introduced by subtracting pairs of images. To do this, we simply double the noise contribution from the background and the read noise (Davison et al. 2014). We determine the SNR for each pixel along the dispersion direction and set the SNR for the spectrum to be the average of these values. The signal to noise is then added in quadrature for the two measurements to give the SNR obtained for the measurement.

### 3.3 Spectroscopic Analysis and Modeling

We fit each observation to a high resolution model that is composed of a synthetic stellar spectrum and an empirical telluric spectrum that are convolved to the resolution of CSHELL. The synthetic stellar spectra are generated from NextGen models (Hauschildt et al. 1999). The telluric model spectra are extracted from observations of the Sun from an ultra high resolution KPNO/FTS telluric spectrum (Livingston & Wallace 1991). We fix the surface gravity, log(g), of the synthetic stellar model to 4.8 dex (cgs) for all of our stars.

The model spectrum consists of 19 free parameters to fit. The linear limb darkening coefficient is set to 0.6 for all stars, which is appropriate for cool stars at infrared wavelengths (Claret 2000). Three of the parameters make up a quadratic polynomial that characterizes the wavelength solution. Nine of the parameters are Gaussians used to model the line spread function (LSF) of the spectrum; we assume that the LSF along the order is constant. The remaining six parameters are the depth of the telluric features, the depth of the stellar features, $v\sin i$, the RV, a normalization constant, and a linear normalization term.

We use the telluric spectrum to solve for the wavelength solution and to characterize the LSF. We then use an iterative process to fit the target spectrum to the model spectrum. On the first iteration, we fit the wavelength solution, the depth of the telluric spectrum, the RV, the normalization constant, and the linear normalization term. With an improved guess on our second iteration, we allow the $v\sin i$, the depth of the telluric model, the depth of spectral model and the two normalization constants to fluctuate. The $v\sin i$ is determined following the description provided in Gray (2005). Finally, we repeat the first iterative process in order to determine the absolute RV of the star. The optimization of the model spectrum is completed using AMOEBA, which is a routine used for minimization of multiple variables using the downhill simplex method of Nelder & Mead (1965).

## 4. $v\sin i$ Results

The $v\sin i$ value is the average value of the two nodded spectra. The error assigned to the $v\sin i$ value is calculated as the standard deviation of the $v\sin i$ measurements for each star.

The spectral resolving power of CSHELL is not high enough to fully resolve the lines of the slowest rotators. Line broadening becomes measurable for $v\sin i$ values in excess of 3 km s$^{-1}$, therefore we set this value as our $v\sin i$ detection limit. Only 13 out of our 65 stars measured in this survey have $v\sin i$ values above our detection limit. Figure .1 shows the fraction of rapidly rotating ($v\sin i > 3$ km s$^{-1}$) mid M-dwarfs (M3-M5.5) in each spectral sub class. This figure includes the 65 new $v\sin i$ measurements and 142 published $v\sin i$ values from the literature. In total, 62 stars of our 207 stars (30%) show rotational broadening of $v\sin i < 3$ km s$^1$. Many of these stars do not have spectroscopically determined or previously published spectral types, therefore we assigned spectral types for statistical uses only to our sample based on their V-K values and classification schemes of Bessell & Brett (1988) and Bessell et al. (1991) and Bessell (1995). We find a lower fraction of rapidly rotating M4.5 dwarfs than Reiners et al. (2012). This hints to an emerging trend that as more $v\sin i$ values in this volume-limited sample of mid M-dwarfs is surveyed that the fraction may continue to decline. This may be a consequence of previous surveys including a higher fraction of young stars, active stars and unknown spectroscopic binaries, as these population of stars tend to be more rapid rotators.

Although it is interesting from a physics perspective to understand the increase in the fraction of stars with $v\sin i$ above 3 km s$^{-1}$, as a large fraction of stars above this limit may indicate that magnetic braking is less efficient for these stars; it is equally interesting to determine the fraction of mid to late M-dwarfs that would be viable targets for low mass planet searches with the radial velocity technique. Barnes et al. (2013) calculates that RV searches with SNR ∼40 can achieve <10 m s$^{-1}$ precision based on simulated photon noise for targets with $v\sin i = 10$ km s$^{-1}$. Using this new criteria of rapid rotation being above 10 km s$^{-1}$, we find ∼92% of mid M-dwarfs (M3-M5.5) and ∼58% of late M-dwarfs (M6-M8) are good candidates for future RV surveys. For an individual break down on the fraction of rapid rotators per spectral class see Figure .2. We do warn that many stars with high rotational velocities may also be active stars. Reiners et al. (2012) finds that all early to mid M-stars with $v\sin i > 3$ km s$^{-1}$ show measurable H$\alpha$. Therefore, stellar jitter might be the limiting factor that determines RV precision.

*Acknowledgments.* The authors are visiting Astronomer at the Infrared Telescope Facility, which is operated by the University of Hawaii under Cooperative Agreement no. NNX-08AE38A with the National Aeronautics and Space Administration, Science Mission Directorate, Planetary Astronomy Program and grateful for the telescope time granted to them. This work was supported by the National Science Foundation through a Graduate Research Fellowship to Cassy Davison. This project is also funded in part by NSF/AAG grant no. 0908018 and the NSF grant no. AST05-07711 and AST09-08402.

## References

Bailey, J. I., White, R. J., Blake, C. H., et al. 2012, ApJ, 749, 16

Barnes, J. R., Jenkins, J. S., Jones, H. R. A., et al. 2013, European Physical Journal Web of Conferences, 47, 5002

Barnes, J. R., Jenkins, J. S., Jones, H. R. A., et al. 2014, MNRAS, 439, 3094

Bessell, M. S., & Brett, J. M. 1988, PASP, 100, 1134

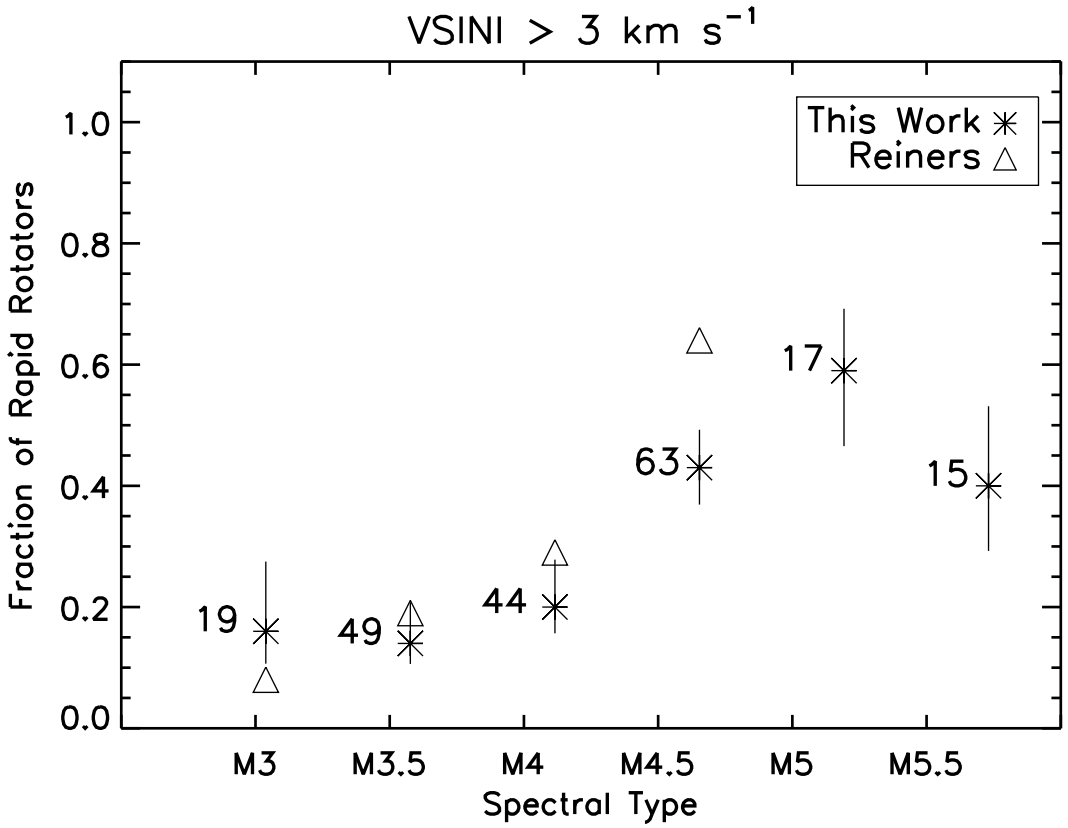


Figure .1: Fraction of rapidly rotating ($v\sin i$ > 3 km s$^{-1}$) stars per spectral type in our sample. This plot includes 65 new $v\sin i$ measurements and 142 literature values. Numbers indicate how many stars are in each per spectral bin. Error bars show 1$\sigma$-uncertainties and are based on binomial statistics. Our sample shows a smaller fraction of rapidly rotating mid M-dwarfs than Reiners et al. (2012).

Bessell, M. S., Brett, J. M., Scholz, M., & Wood, P. R. 1991, A&AS, 89, 335

Bessell, M. S. 1995, PASP, 107, 672

Browning, M. K., Basri, G., Marcy, G. W., West, A. A., & Zhang, J. 2010, AJ, 139, 504

Bonfils, X., Delfosse, X., Udry, S., et al. 2013, A&A, 549, A109

Claret, A. 2000, A&A, 363, 1081

Davison, C, et al., in prep

Davison, C. L., White, R. J., Jao, W.-C., et al. 2014, AJ, 147, 26

Delfosse, X., Forveille, T., Perrier, C., & Mayor, M. 1998, A&A, 331, 581

Dressing, C. D., & Charbonneau, D. 2013, ApJ, 767, 95

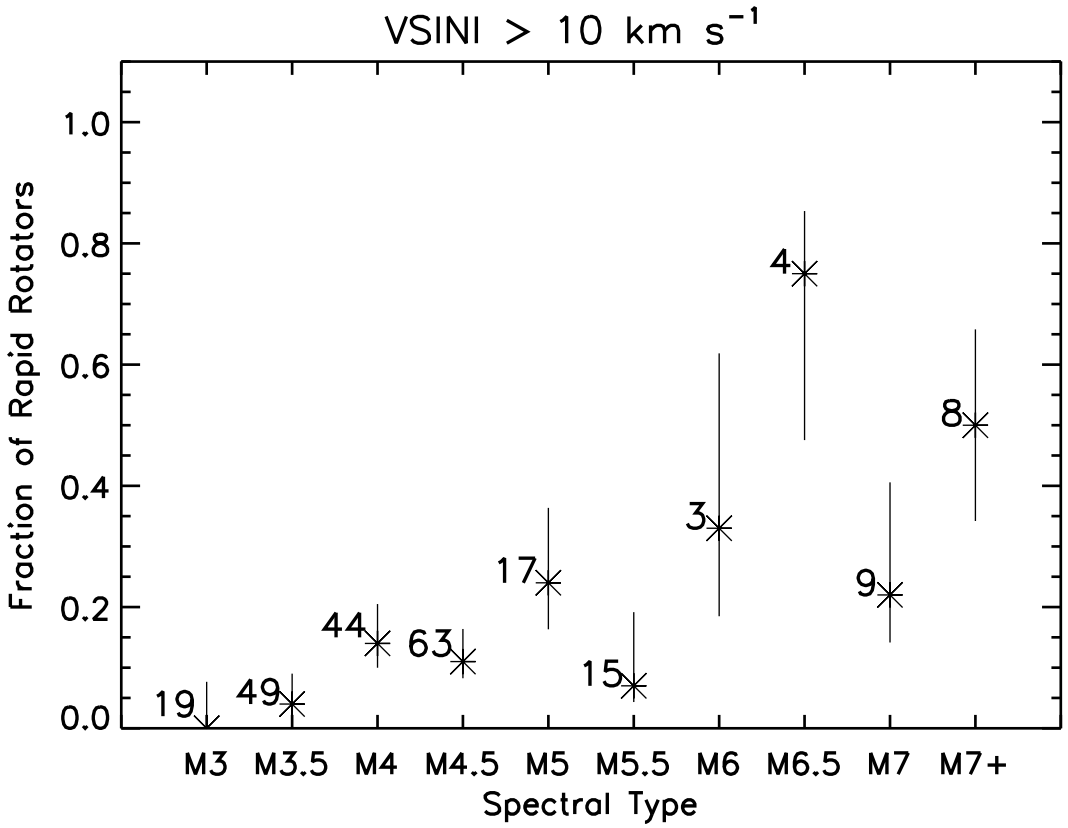


Figure .2: Fraction of rapidly rotating ($v\sin i$ > 10 km s$^{-1}$) stars per spectral type in our sample. This includes 65 new $v\sin i$ measurements and 166 literature values. Numbers indicate how many stars are measured per spectral bin. Error bars show 1$\sigma$-uncertainties and are based on binomial statistics. We find ∼92% of mid M-dwarfs (M3-M5.5) and ∼58% of late M-dwarfs (M6-M8) have $v\sin i$ values below 10 km s$^{-1}$.

Gray, D. F. 2005, PASP, 117, 711

Greene, T. P., Tokunaga, A. T., Toomey, D. W., & Carr, J. B. 1993, Proc. SPIE, 1946, 313

Henry, T. J., Jao, W.-C., Pewett, T., et al. 2014, American Astronomical Society Meeting Abstracts #224, 224, #120.26

Hauschildt, P. H., Allard, F., & Baron, E. 1999, ApJ, 512, 377

Horne, K. 1986, PASP, 98, 609

Jenkins, J. S., Ramsey, L. W., Jones, H. R. A., et al. 2009, ApJ, 704, 975

Jones, H. R. A., Pavlenko, Y., Viti, S., et al. 2005, MNRAS, 358, 105

Livingston, W., & Wallace, L. 1991, NSO Technical Report, Tucson: National Solar Observatory, National Optical Astronomy Observatory, 1991,

Mahadevan, S., Ramsey, L., Bender, C., et al. 2012, PROC. SPIE, 8446,

Marcy, G. W., & Chen, G. H. 1992, ApJ, 390, 550

Mohanty, S., & Basri, G. 2003, ApJ, 583, 451

Mortara, L., & Fowler, A. 1981, PROC. SPIE, 290, 28

Nelder, J.A., & Mead, R. 1965, Computer Journal, 7, 308

Quirrenbach, A., Amado, P. J., Mandel, H., et al. 2010, Pathways Towards Habitable Planets, 430, 521

Rayner, J., Bond, T., Bonnet, M., et al. 2012, PROC. SPIE, 8446,

Reiners, A., & Basri, G. 2007, ApJ, 656, 1121

Reiners, A., & Basri, G. 2008, ApJ, 684, 1390

Reiners, A., & Basri, G. 2010, ApJ, 710, 924

Reiners, A., Joshi, N., & Goldman, B. 2012, AJ, 143, 93

Reshetov, V., Herriot, G., Thibault, S., et al. 2012 PROC. SPIE, 8446,

Stauffer, J. B., & Hartmann, L. W. 1986, PASP, 98, 1233

Swift, J. J., Johnson, J. A., Morton, T. D., et al. 2013, ApJ, 764, 105

Tanner, A., White, R., Bailey, J., et al. 2012, ApJS, 203, 10

Tokunaga, A. T., Toomey, D. W., Carr, J., Hall, D. N. B., & Epps, H. W. 1990, PROC. SPIE, 1235, 131